Charge carrier concentration and structural transition temperatures in Heusler alloys $Ni_{50}Mn_{36}Sb_{14-x}Z_x$ (Z = Al, Ge; x = 0; 1; 2; 3; 4)

Charge carrier concentration and structural transition temperatures in Heusler alloys $Ni_{50}Mn_{36}Sb_{14-x}Z_x$ (Z = Al, Ge; x = 0; 1; 2; 3; 4)

S M Emelyanova[1], T V Dyachkova[2], A P Tyutyunnik[2], V V Chistyakov[1], A N Domozhirova[1], F Sauerzopf[3], R L Wang[4], C Yang[4] and V V Marchenkov[1,5]

[1] M.N. Mikheev Institute of Metal Physics, UB RAS, Ekaterinburg, 620137, Russia
[2] Institute of Solid State Chemistry, UB RAS, Ekaterinburg, 620990, Russia
[3] TU Wien, Atominstitute, Vienna, 1020, Austria
[4] Hubei University, Wuhan, 430062, China
[5] Ural Federal University, Ekaterinburg, 620002, Russia

E-mail: emelyanova@imp.uran.ru, march@imp.uran.ru

Abstract. The temperature dependences of magnetization and electrical resistance of the $Ni_{50}Mn_{36}Sb_{14-x}Z_x$ (Z = Al, Ge; x = 0; 1; 2; 3; 4) alloys have been used to determine the structural transition temperatures (STT) such as: M_s, M_f, A_s and A_f (temperatures of the start and finish of martensitic and austenitic transformations, respectively). Effect of various parameters (e/a, V_{cell}, n) on the STT was studied. Using Hall Effect the concentration of charge carriers n* was obtained and it was found that n* is not strongly correlated with a behaviour of STT, there is only a general trend with exceptions.

1. Introduction

Traditionally, gadolinium used as a material for the working body in solid-state magnetic refrigerators. However recently so-called shape-memory ferromagnets have become increasingly an alternative, since these alloys can exceed compounds with gadolinium in the value of MCE (magnetocaloric effect) for magnetic field of the same magnitude [1]. Giant values of the MCE are achieved in them due to the structural transformation accompanying the magnetic transition.

There are two main parameters affecting the STT: the ratio e/a (the number of valence electrons per atom) and the volume of the unit cell (V_{cell}). In the first case, a direct relationship is observed: the STT increase as e/a increases, and in the second case, the relationship is inverse: as the V_{cell} decreases, the temperatures increase (for example, the relationship between STT and V_{cell} is true for the Ge-doped alloys Ni-Mn-Sn [2], H-doped alloys Ni-Mn-In [3]). However, these trends are not always traced. It was reported about non-monotonic dependence of M_s on e/a in $Ni_{50}Mn_{35-x}Cu_xSn$ [4] and $Ni_{2-x}Cu_xMnGa$ [5]. In particular, in [6] it is indicated that the ratio e/a in $Ni_{48}Mn_{39}Sn_{13-x}Si_x$ system alloys ($1 \leq x \leq 4$) does not change with an increase in the Si content and is constantly equal to 8.05; however, the M_S temperature decreases. In addition, for the Ni-Mn-Ga [7] and Ni-Mn-In-Sb systems [8], it was found that the STT decrease even if the substitution leads to an increase in the e/a ratio and a decrease in the V_{cell}.

The purpose of this work is to study the Hall Effect, obtaining the concentration of current carriers n*, and looking for the correlation between n* and the STT in Heusler-like alloys $Ni_{50}Mn_{36}Sb_{14-x}Z_x$ (Z = Al, Ge; x = 0; 1; 2; 3).

2. Experimental

Ingots were prepared by arc melting in an inert atmosphere and subsequently subjected to annealing at 1100 K for 24 h followed by furnace cooling. Samples for magnetization measurements were cut from preparing ingots by spark cutting. The elemental analysis was performed using an Inspect F scanning electron microscope (FEI Company, USA) equipped with a field-emission cathode and an EDAX spectrometer. The accuracy of elemental analysis is ±2 rel. %. The structural analysis was performed at the Collaborative Access Center, M.N. Mikheev Institute of Metal Physics, UB RAS. X-ray diffraction studies were performed in the Laboratory of Structural Phase Analysis at the Institute of Solid State Chemistry, UB RAS. A STADI-P (STOE, Germany) powder auto diffractometer and CuK_α (wave length is λ = 1.542 Å) were used. X-ray diffraction patterns were taken at room temperature in an angular range of 5°-120°. The magnetic and galvanomagnetic properties were measure at the Atomistitut, TU Wien using an MPMS XL7 (Quantum Design) SQUID magnetometer. The magnetic properties were measured in magnetic fields of up to 10 kOe in the temperatures range 150-330 K. The Hall Effect were measured by the standard dc four-probe method for the temperature 4.2 K and in magnetic fields of up to 100 kOe.

3. Results and discussion

The STT were determined from the temperature dependences of the magnetization and electrical resistance using the method of tangens [9, 10], according to which this temperatures were determined at their intersection (table 1). It is obvious that for all alloys doping with germanium, the STT is lower than in the original ternary compound $Ni_{50}Mn_{36}Sb_{14}$, and the temperatures decrease as the germanium content in the alloy increases. The only exception is the alloy $Ni_{50}Mn_{36}Sb_{13}Ge_1$, which is demonstrates STT superior to those for the original alloy. In aluminium doping alloys a completely different tendency can be traced, the STT, on the contrary, exceed to those for the alloy $Ni_{50}Mn_{36}Sb_{14}$, and increase as the aluminium content increases.

Table 1. Structural transition temperatures (K), ratio e/a and charge carrier concentration n* for the $Ni_{50}Mn_{36}Sb_{14-x}Z_x$ (Z = Al, Ge; x = 0; 1; 2; 3; 4) alloys. The temperatures of the start and finish of martensitic transformation are designated as M_s and M_f respectively; the temperatures of the start and finish of austenitic transformation are A_s and A_f, respectively.

Alloy	A_s	A_f	M_s	M_f	e/a	$n^* \cdot 10^{23}$, $1/cm^3$
$Ni_{50}Mn_{36}Sb_{11}Ge_3$	207	214	202	197	8.19	0.13
$Ni_{50}Mn_{36}Sb_{12}Ge_2$	218	224	216	209	8.20	0.43
$Ni_{50}Mn_{36}Sb_{13}Ge_1$	205	246	237	212	8.21	0.18
$Ni_{50}Mn_{36}Sb_{14}$	231	238	232	225	8.22	0.48
$Ni_{50}Mn_{36}Sb_{13}Al_1$	237	240	234	229	8.20	0.21
$Ni_{50}Mn_{36}Sb_{12}Al_2$	264	273	264	258	8.18	0.07
$Ni_{50}Mn_{36}Sb_{10}Al_4$	282	306	300	274	8.14	0.19

The calculation of e/a was carried out according to the equation (1) below [11] as the sum of the products of the number of valence d- and s-electrons of the chemical element including in the alloy, on the fraction of this chemical element:

$$\frac{e}{a} = (C_A \cdot Z_A) + (C_B \cdot Z_B) + (C_D \cdot Z_D), \quad (1)$$

where C_A, C_B, C_D – concentrations of elements A, B, D; Z_A, Z_B, Z_D – the number of external (valence) electrons for the elements A, B, D. The number of valence electrons was assumed to be 10, 7, 5, 4 and 3 for Ni ($3d^84s^2$), Mn ($3d^64s^1$), Sb ($5s^25p^3$), Ge ($4s^24p^2$) and Al ($3s^23p^1$), respectively.

For alloys containing germanium, it was found that lowering ratio e/a leads to a decrease in STT. In alloys containing aluminium, the situation is completely opposite: with decreasing e/a STT increases, although between them there should be a direct relationship. It should be noted that the $Ni_{50}Mn_{36}Sb_{12}Ge_2$ and $Ni_{50}Mn_{36}Sb_{13}Al_1$ alloys have the same value of e/a, but their STT differs significantly. Thus, it becomes obvious that the ratio e/a is not sufficient to describe the behavior of STT, especially in four-component systems, a similar conclusion was made in [12].

The results of x-ray studies of the $Ni_{50}Mn_{36}Sb_{12}Ge_2$ alloy are shown in figure 1. It can be seen that the sample is single-phase (all reflections correspond to the same structural type), i.e., the sample contains 100 % compound with the Ni_2MnSb-type (the lattice parameters is a = 5.957 Å). Other alloys contain an irrelevant small amount of secondary phases: $Ni_{50}Mn_{36}Sb_{14}$ alloy sample contain 1.9 wt %Ni_3Sb, $Ni_{50}Mn_{36}Sb_{12}Al_2$ alloy sample contain 10.3 wt % MnAl and 1.3 wt % Ni_3Sb. Since the content of the secondary phases is insignificant, in the present work it was assumed that all alloys are in the austenitic state. From the x-ray studies V_{cell} was determined. As an example, table 2 shows the values of the V_{cell} for some of the studied alloys. It was found that a decrease in the V_{cell} does not lead to an increase in STT, on the contrary, they decreases. It was expected that the alloy $Ni_{50}Mn_{36}Sb_{12}Ge_2$ will show the highest values of STT, since it has the lowest value of V_{cell} = 211.29 $Å^3$. The highest STT values are characteristic for alloy $Ni_{50}Mn_{36}Sb_{12}Al_2$ despite the fact that the V_{cell} for this alloy is 212.35 $Å^3$.

Table 2. Values of the V_{cell} and density of valence electrons n for the alloys $Ni_{50}Mn_{36}Sb_{14-x}Z_x$ (Z = Al, Ge; x = 0; 2).

Alloy	V_{cell}, $Å^3$	n, $1/cm^3$
$Ni_{50}Mn_{36}Sb_{12}Ge_2$	211.29	$62.09 \cdot 10^{22}$
$Ni_{50}Mn_{36}Sb_{14}$	213.95	$61.47 \cdot 10^{22}$
$Ni_{50}Mn_{36}Sb_{12}Al_2$	212.35	$61.63 \cdot 10^{22}$

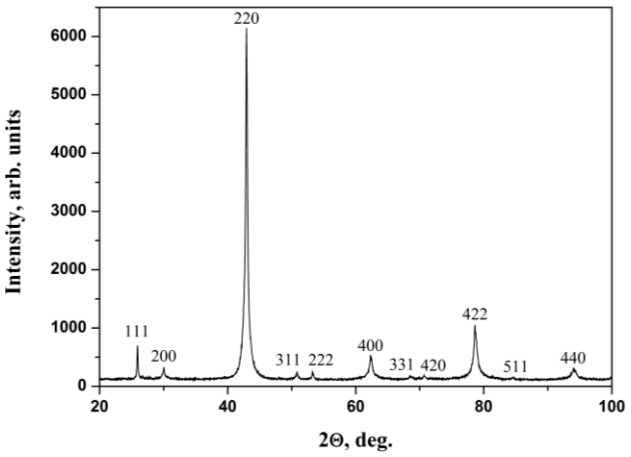

Figure 1. X-ray diffraction pattern of the $Ni_{50}Mn_{36}Sb_{12}Ge_2$ alloy.

In addition, the definition of V_{cell} can be complicated by the fact that the structural transformation in the alloy has not yet been completed, and therefore the phase composition is represented by a mixture of martensite and austenite. It becomes obvious that the V_{cell} as well as the ratio e/a cannot reliably describe the behavior of STT.

In accordance with the above, varying the density of valence electrons n can be considered as a way to influence STT. This approach was implemented in [13] for alloys of the Ni-Mn-Ga system, the density of valence electrons was calculated with equation (2):

$$n = \frac{\left(\frac{e}{a}\right) \cdot n_1}{V_{cell}}, \quad (2)$$

where n_1 is the average number of atoms per unit cell (for alloys of the systems Ni-Mn-Z (Z = Ga, In, Sb, Sn) it is 16).

It was assumed, that as the parameter n increases, the STT should also increase, but this does not occur in the studied alloys. For the alloys $Ni_{50}Mn_{36}Sb_{14}$ and $Ni_{50}Mn_{36}Sb_{12}Al_2$ difference between the values of the parameter n is not significant: $61.47 \cdot 10^{22}$ 1/cm^3 and $61.63 \cdot 10^{22}$ 1/cm^3, respectively. However, the STT values for these alloys are differ significantly from each other. For example, the M_s (start temperature of martensitic transformation) for alloy $Ni_{50}Mn_{36}Sb_{14}$ equal to 232 K, and for alloy $Ni_{50}Mn_{36}Sb_{12}Al_2$ – 264 K. Alloy $Ni_{50}Mn_{36}Sb_{12}Ge_2$ has the lowest values of STT, despite parameter n is $62.09 \cdot 10^{22}$ 1/cm^3.

Thus, the correlation between the STT and the above mentioned parameters (e/a, V_{cell}, n) is not always fulfilled. Since during structural transformations, a change in the electronic structure also occurs, one can try to find a correlation between the parameters of the electronic subsystem and the STT. One of such parameters is the concentration of charge carriers, determined, e.g., from the Hall Effect measurements.

The field dependences of the Hall resistivity $\rho_H(H)$ and the magnetization curves (obtained at 4.2 K) have the same general view. The curves $\rho_H(H)$ and M(H) have two distinguishable intervals of magnetic fields, such as the technical magnetization region (H < 10 kOe), and the paraprocess region at higher fields. Taking into account the fact that for $\rho_H(H)$ and M(H) curves there are no saturation effect and linear dependence even in strong magnetic fields, we used the approach proposed in [14]. The coefficients R_0 and R_S were determined from the dependences $\rho_H(H)$ and M(H) in the paraprocess region with the equation (3):

$$\frac{\rho_H}{H} = R_0 + \frac{4\pi R_S^* M}{H}, \quad (3)$$

where $R_S^* = R_S + (1-N)R_0$, N – demagnetization factor. The first term in equation (3) describes the normal Hall Effect (NHE), which in metals is caused by the Lorentz force on the charge carriers and is proportional to the applied magnetic field. The second term in equation (3) is determined by so-called anomalous Hall Effect (AHE).

From the figure 2 it can be seen that equation (3) is valid for $\rho_H(H)$ and M(H) of all investigated alloys in the limit of strong magnetic fields (H > 10 kOe).

The NHE coefficient R_0 is characterized by the number n* of current (charge) carriers per unit specimen volume with equation (4):

$$R_0 = \frac{1}{n^* ec}, \quad (4)$$

where c is the light velocity, e is the charge of a current carrier. In the present work for $Ni_{50}Mn_{36}Sb_{14-x}Z_x$ (Z = Al, Ge; x = 0; 1; 2; 3; 4) alloys the coefficient of the NHE was determined and then the number of charge carriers n* was calculated, obtained values are given in table 1. In all cases the coefficient of NHE is positive, therefore, in the studied alloys the main charge carriers are holes.

It should be noted that the Fermi surface of Heusler alloys has a complex topology and contains the various sheets of both electronic and hole types. Therefore, to accurately determine the concentration of current carriers, it is necessary to have the data on Fermi surface topology of certain alloy, as well as the data on the mobility of charge carriers belonging to certain sheets of the Fermi surface. This is quite a challenge. However, as shown in [15-20], estimating the concentration of current carriers using one band model makes it possible to qualitatively track the changes in the electronic characteristics

and qualitatively determine the correlation between them even in such complex compounds. Therefore, we also use one band model.

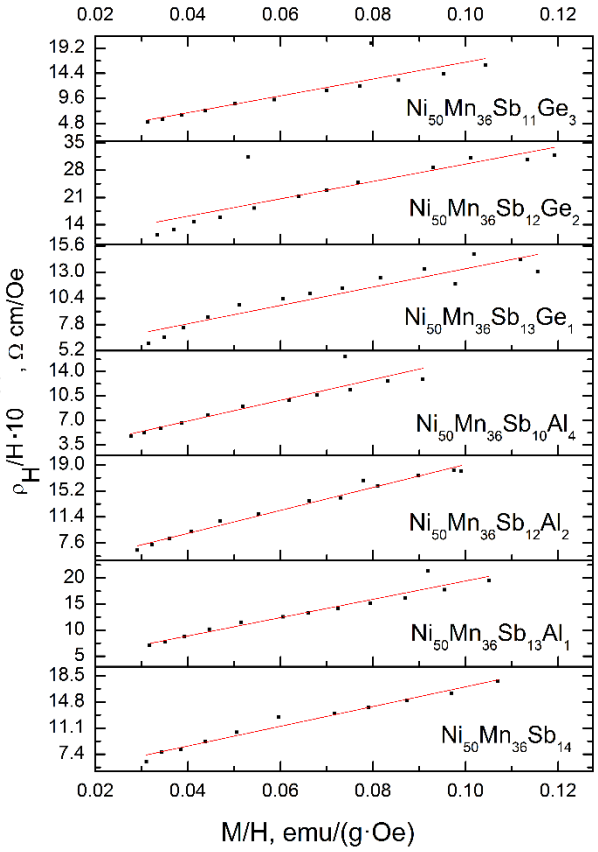

Figure 2. Dependences ρ_H/H on M/H for alloys $Ni_{50}Mn_{36}Sb_{14-x}Z_x$ (Z = Al, Ge; x = 0; 1; 2; 3; 4).

Figure 3 shows the dependences STT on n* for all investigated alloys. It is obvious that aluminium-doped alloys exhibit higher STT values compared to the initial ternary compound $Ni_{50}Mn_{36}Sb_{14}$. Germanium-doped alloys, on the contrary, demonstrate lower STT than the initial compound. This fact is especially pronounced for A_s and M_f. Temperatures M_s and A_f for alloys doped by 1 at.% of Al or Ge and $Ni_{50}Mn_{36}Sb_{14}$ are almost the same. Probably the reason for this is a small amount of alloying element. Alloy $Ni_{50}Mn_{36}Sb_{14}$ has the highest value of n* equal to $0.48 \cdot 10^{23}$ 1/cm^3.

Values of n* for alloys doped by 1; 2 and 4 at% of Al is $0.21 \cdot 10^{23}$; $0.07 \cdot 10^{23}$; $0.19 \cdot 10^{23}$ 1/cm^3, respectively. M_s for alloy $Ni_{50}Mn_{36}Sn_{14}$ is 232 K, for alloy $Ni_{50}Mn_{36}Sb_{13}Al_1$ – 234 K. In the future this tendency will continue, e.g., as n* decreases values of M_s will increase: for alloy $Ni_{50}Mn_{36}Sb_{10}Al_4$ M_s is 300 K. The value of n* was expected to be higher than 300 K, but it is 264 K. It is obviously that this dependence is not continue, a similar situation is also observed for M_f, A_s and A_f. For the alloys doped by Ge, in general, a different trend is observed: as n* decreases values of M_s will decrease too, more exactly, for alloy $Ni_{50}Mn_{36}Sb_{12}Ge_2$ M_s = 216 K, for alloy $Ni_{50}Mn_{36}Sb_{11}Ge_3$ – 202 K. The exception is the alloy $Ni_{50}Mn_{36}Sb_{13}Ge_1$ for which n* = $0.18 \cdot 10^{23}$ 1/cm^3 and M_s = 237 K.

It should be noted that alloys $Ni_{50}Mn_{36}Sb_{14}$ and $Ni_{50}Mn_{36}Sb_{12}Ge_2$ have approximately the same values of n*: $0.48 \cdot 10^{23}$ and $0.43 \cdot 10^{23}$ 1/cm^3, but M_s for this alloys is differ: 232 and 216 K, respectively. Values of n* for alloys $Ni_{50}Mn_{36}Sb_{10}Al_4$ and $Ni_{50}Mn_{36}Sb_{13}Ge_1$ are also close in meaning ($0.19 \cdot 10^{23}$; $0.18 \cdot 10^{23}$ 1/cm^3), however values of M_s for this alloys are significantly differ in meaning: 300 and 237 K, respectively.

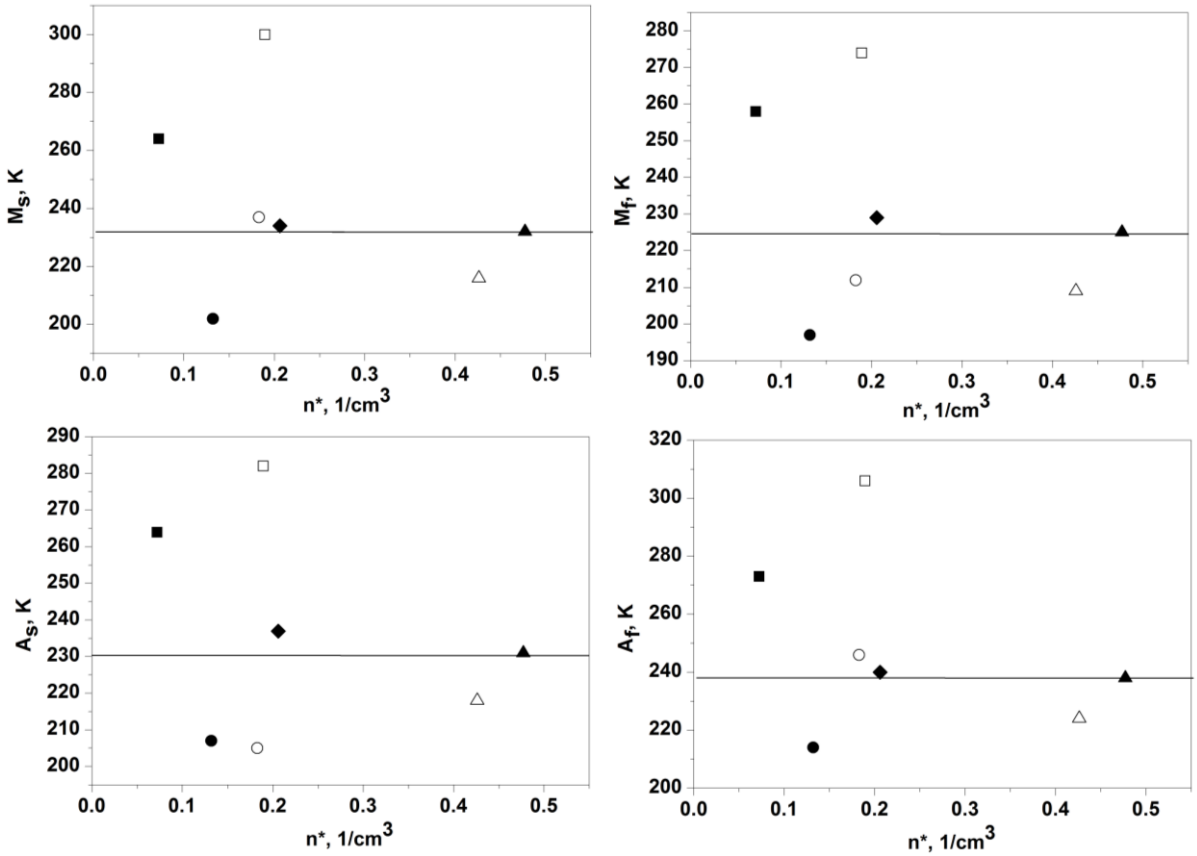

Figure 3. Dependence STT on charge carrier concentration: ▲ – $Ni_{50}Mn_{36}Sb_{14}$, ♦ - $Ni_{50}Mn_{36}Sb_{13}Al_1$, ■ - $Ni_{50}Mn_{36}Sb_{12}Al_2$, □ - $Ni_{50}Mn_{36}Sb_{10}Al_4$, ○ - $Ni_{50}Mn_{36}Sb_{13}Ge_1$, Δ - $Ni_{50}Mn_{36}Sb_{12}Ge_2$, ● - $Ni_{50}Mn_{36}Sb_{11}Ge_3$. The horizontal line passes through temperatures corresponding to the initial ternary compound $Ni_{50}Mn_{36}Sb_{14}$.

4. Conclusions

The magnetization, the electrical resistivity and the Hall Effect of $Ni_{50}Mn_{36}Sb_{14-x}Z_x$ (Z = Al, Ge; x = 0; 1; 2; 3; 4) Heusler alloys were measured at temperatures from 150 K to 330 K and in magnetic fields of up to 10 kOe. The V_{cell}, the e/a parameter, the density of valence electrons n, and the charge carriers concentration n* were determined. An attempt to find a correlation between STT and above mentioned parameters were made. It was shown that this correlation is not strongly, there is only a general trade.

Acknowledgements

The results of this work were obtained within the state assignment of Minobrnauki of Russia (theme "Spin" No. AAAA-A18-118020290104-2) and "New functional materials for promising technologies: synthesis, properties, spectroscopy and computer simulation" (No. AAAA-A19-119031890025-9), supported in part by RFBR grant (project No. 18-02-00739).

References

[1] Liu J, Gottoschall T, Skokov K P, Moore J D and Gutfleisch O 2012 *Nature Mater.* **11** 620
[2] Han Z D, Wang D H, Zhang C L, Xuan H C, Zhang J R, Gu B X and Du Y W 2009 *Mater. Sci. Eng.* B **157** 40
[3] Hu F X, Wang J, Chen L, Zhao J L, Sun J R and Shen B G 2009 *Appl. Phys. Lett.* **95** 112503
[4] Gao B, Shen J, Hu F X, Wang J, Sun J R and Shen B G 2009 *Appl. Phys.* A **97** 443

[5] Kanomata T, Nozawa T, Kikuchi D, Nishihara H, Koyama K and Watanabe K 2005 *Int. J. Appl. Electromagn. Mech.* **21** 151
[6] Muthu S E, Singh S, Thiyagarajan R, Selvan G K, Rama Rao N V, Raja M M and Arumugam S 2013 *J. Phys. D: Appl. Phys.* **46** 205001
[7] Liu Z H, Zhang M, Wang W Q, Wang W H, Chen J L, Wu G H, Meng F B, Liu H Y, Liu B D, Qu J P and Li Y X 2002 *J. Appl. Phys.* **92** 5006
[8] Liu Z, Wu Z, Yang H, Liu Y, Liu E, Zhang H and Wu G 2010 *Intermetallics* **18** 1690
[9] Monograph edited by Prof. Pushin V G 2006 *Shape memory titanium nickelide alloys C I Structure, phase transformators and properties* (Ekaterinburg: Ural Branch of RAS) p 438
[10] Pogodin-Alekseev G I 1950 *Metal science. Analysis methods, laboratory works and tasks* (Moscow: State publishing house of defense industry) p 458
[11] Kan R 1967 *Physical metallurgy* (Moscow: Mir) p 624
[12] Comtesse D, Gruner M E, Sokolovsky V V, Buchelnikov V D, Grunebohm A, Arroyave R, Singh N, Gottschall T, Gutfleisch O, Chernenko V, Albertini F, Fahler S and Entel P 2014 *Phys. Rev.* B **89** 184403
[13] Chen X Q, Yang F J, Lu X and Qin Z X 2007 *Phys. Stat. Sol.* (b) **3** 1047
[14] Kourov N I, Marchenkov V V, Perevozchikova Yu A and Weber H W 2017 *Phys. Solid State* **59** 63
[15] Kourov N I, Marchenkov V V, Belozerova K A and Weber H W *2015 J. Exp. Theor. Phys.* **121** 844
[16] Kourov N I, Marchenkov V V, Korolev A V, Lukoyanov A V, Shirokov A A and Perevozchikova Yu A 2017 *Materials Research Express* **4** 116102
[17] Marchenkov V V, Perevozchikova Yu A, Kourov N I, Irkhin V Yu, Eisterer M and Gao T 2018 *J. Magn. Magn. Mater.* **459** 211
[18] Marchenkov V V, Kourov N I and Irkhin V Yu 2018 *Physics of Metals and Metallography* **119** 1321
[19] Marchenkov V V, Irkhin V Yu, Perevozchikova Yu A, Terent'ev P B, Semiannikova A A, Marchenkova E B and Eisterer M 2019 *J. Exp. Theor. Phys.* **128** 919
[20] Perevozchikova Yu A, Semiannikova A A, Domozhirova A N, Patrakov E I, Eisterer M, Korenistov P S and Marchenkov V V 2019 *Low Temp. Phys.* **45** 015907